

## Mn<sup>2+</sup> ions retention onto agriculture waste: a statistical design analysis, estimation of equilibrium and kinetic parameters

Saeed Mirani<sup>a</sup>, Narges Samadani Langeroodi<sup>a,\*</sup>, Alireza Goudarzi<sup>b</sup>, Pouneh Ebrahimi<sup>a</sup>

<sup>a</sup>Department of Chemistry, Golestan University, Gorgan, Iran, email: s.mirani69@gmail.com (S. Mirani), nsamadani@yahoo.com (N.S. Langeroodi), epouneh@yahoo.com (P. Ebrahimi)

<sup>b</sup>Faculty of Polymer Engineering, Golestan University, Gorgan, Iran, email: goudarzi.alireza@gmail.com

Received 15 June 2016; Accepted 13 December 2016

### ABSTRACT

This paper describes the adsorption of Mn<sup>2+</sup> ions from aqueous solution by the Iranian oak-fruit shell as low-cost adsorbent. The effect of various parameters such as pH of solution, contact time, initial Mn<sup>2+</sup> concentration and adsorbent weight for the adsorptive retention process were investigated. SPSS software was employed for prediction and investigation of factor importance in determining of removal ratio of Mn<sup>2+</sup>. According to Beta-value the importance order of factors is: pH of solution, adsorbent weight, initial Mn<sup>2+</sup> concentration and time, respectively. In process optimization, removal ratio of Mn<sup>2+</sup> was achieved as 73.59% with a pH of 5.0, contact time of 210 min, initial Mn<sup>2+</sup> concentration of 10 mg/L, and adsorbent weight of 2.5 g. Also, the obtained results from this study show the good adaptation between experimental and prediction values of removal ratio of Mn<sup>2+</sup>. Equilibrium studies show that Mn<sup>2+</sup> adsorption data follow Freundlich model. Pseudo-second-order kinetic model agrees very well with the experimental data. The desorption and regeneration studies have proven that adsorbent can be potentially reused for further adsorption process. Fourier transform infrared spectroscopy (FTIR spectra) and scanning electron microscope (SEM) were used to characterize the biosorbent.

*Keywords:* Biosorbent; Oak-fruit shell; Statistical analysis; Manganese; Isotherm; Kinetics

### 1. Introduction

Contamination of aquatic environment with heavy and toxic metals is a complex problem and their removal requires much attention. Heavy metals such as chromium, copper, lead, cadmium, etc., in wastewater are toxic and unlike most organic contaminants, they are not biodegradable in the environment. Because of their toxicity, their pollution effect on our ecosystem presents a possible human health risk [1–4]. Numerous methods are currently employed to remove heavy metals from industrial effluent, including chemical oxidation and reduction, liquid extraction, ion exchange, membrane separation, crystallization, reverse osmosis and electro-dialysis. However, most

of these techniques either strongly depend on concentration of pollutants, or lack practical applications because of economic constraints. Adsorption is one alternative method for such cases and is an effective purification and separation technique. In recent years, activated carbon prepared from biomaterials and a number of naturally available, low-cost and effective adsorbents have been successfully employed as adsorbent for removing various kinds of metal cations and dyes from wastewater [5–9]. In this study, Iranian oak-fruit shell has been used as adsorbent. Oak tree grows in the forests of northern Iran. In Iran mainly, oak fruit is used for animal feed. To our knowledge, no similar report about of OFS applied to removal of Mn<sup>2+</sup> ions from aqueous solution is available up to now. It has long been known that Mn is one of the most widely used metals in

\*Corresponding author.

the world and one of the important indexes of the water pollutants. Manganese primarily exists in the form of divalent manganese cation ( $Mn^{2+}$ ) in drinking water. In neutral and alkaline environments,  $Mn^{2+}$  is difficult to be oxidized. As an essential element for humans, animals and plants, Mn is required for their growth, development, and maintenance of health. However, excessive concentrations of Mn could result in metallic tasting water and many health problems. The recommended limit in drinking water is 0.05 mg/L and between 0.01 and 0.02 mg/L in water meant for industrial purpose. It has been implicated for neurological disorder when inhaled at a rate of about 10 mg/d [10,11]; thus, there is a need for effective removal of  $Mn^{2+}$  from its aqueous solution. A wide range of adsorbents have been developed and tested for removal of  $Mn^{2+}$  from its aqueous solution, including sargassum biomass [9], polyvinyl alcohol/chitosan (PVA/CS) [11], Co/Mo layered double hydroxide (Co/Mo-LDH) [12], activated carbon from coconut shells [13], aerobic activated sludge and anaerobic activated sludge [14], enhanced empty fruit bunch (EFB) [15], and white rice husk ash [16].

In this research work, we used oak-fruit shell as biosorbent to remove  $Mn^{2+}$  ions from aqueous solution. This biosorbent was examined by IR, and SEM. Batch adsorption studies were performed to evaluate the effect of various parameters such as pH of solution, contact time, initial  $Mn^{2+}$  concentration and adsorbent weight for the adsorptive retention process. SPSS software was employed for prediction of factor importance. A theoretical model was introduced for investigation of factor importance in determining of the removal ratio of  $Mn^{2+}$ . Optimal parameters obtained by this software. In the optimum conditions, adsorption isotherms, reaction kinetics and adsorbent regeneration were investigated.

## 2. Materials and methods

### 2.1. Batch studies

The chemicals used during this study were purchased from Chem-Lab NV(Belgium). Oak fruit which were collected from the forests of northern Iran (Alangdareh) was washed with deionized water and later dried in an oven at 333.15 K. Then, the shell was separated from it. In the following, the dried OFS grounded into smaller particles using a mechanical grinder (Cutting mill-pulverisette 15) and was then crushed using a crushing mill (Fritsch, Germany) of type planetary ball mill PM 5. The powder then was stored in desiccator before being used in the experiments. A stock solution of manganese (1000 mg/L) was prepared in deionized double distilled water using manganese nitrate. All working solutions of varying concentrations (10–50 mg/L) were obtained by successive dilution. All the experiments were performed in 250 cm<sup>3</sup> conical flasks containing 200 cm<sup>3</sup> solutions in each flask under a constant temperature shaker with a shaking of 150 rpm. The pH of the solution was adjusted to required value by adding either 1 M HCl or 1 M NaOH using pH meter (Model Metron, 827 pH Lab). About 200 cm<sup>3</sup> of the experimental solutions was mixed with 1 g of OFS in stopped conical flasks (1 g/200 cm<sup>3</sup>) and the suspensions were equilibrated by shaking for

a desired period of time. The clear supernatants after filtration were analyzed for manganese ion concentrations using an Atomic Absorption Spectrometer (Model Shimadzu, AA-7000). The removal ratio of  $Mn^{2+}$  was calculated using the following equation:

$$\eta = \frac{C_0 - C_e}{C_0} \times 100 \quad (1)$$

where  $C_0$  (mg/L) and  $C_e$  (mg/L) are the initial and equilibrium concentrations of the adsorbate, respectively and  $\eta$  is the removal ratio (in percent) of  $Mn^{2+}$ .

The FTIR spectra analysis of the biosorbent used in this study was characterized with a FTIR (Perkin-Elmer Model System 2000 using KBr pellet method). In order to directly observe the surface morphology of the biosorbent, SEM (Scanning Electron Microscopy) (JSM-5900LV, Japan) was employed in this study.

### 2.2. Desorption of adsorbent

HCl was used to investigate the leaching/desorption of  $Mn^{2+}$  from OFS. After adsorption in optimal conditions, the  $Mn^{2+}$ —adsorbed OFS was filtered and stirred for 5 min with 10 mL of HCl (1 mol/L). After filtration, washed and was then dried at 50°C. At this time the adsorbent prepared, was used again in the optimum conditions for adsorption of  $Mn^{2+}$  from aqueous solution.

## 3. Results and discussion

### 3.1. Effect of adsorbent weight and initial concentration at fixed contact time

The effects of adsorbent weight on the removal ratio of  $Mn^{2+}$  (for minimum and maximum concentrations 10 and 50 mg/L) were showed in Fig. 1. It could be seen from the figure that the removal ratio increased gradually with increasing adsorbent weight, to a maximum 4 g. After this maximum equilibrium value, the removal ratio did not increase with increasing adsorbent weight. These results suggest that the relationship between adsorbent weight and removal ratio

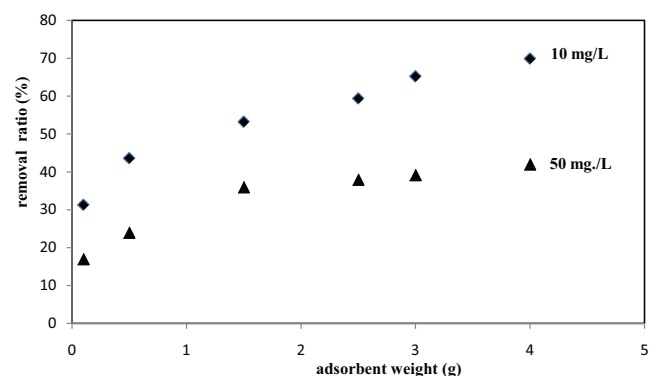


Fig. 1. Effect of adsorbent weight and initial concentration (for minimum and maximum concentrations 10 and 50 mg/L) on removal ratio of  $Mn^{2+}$  ions at room temperature ( $t = 4$  h).

was related to increase in the number of adsorption sites, and that increasing this number had no effect after equilibrium was reached.

Fig. 1 shows as the initial  $Mn^{2+}$  concentration increases (for a certain weight of adsorbent), the removal ratio decreases. Sufficient adsorption sites are available at lower initial concentration, but at higher concentration metal ions are greater than adsorption sites.

From the results, the minimum and maximum weight of adsorbent was determined (0.1 and 4 g).

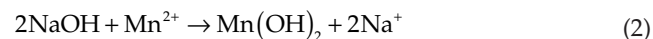
### 3.2. Effect of contact time and initial concentration at fixed adsorbent weight

Fig. 2 represents the adsorption of  $Mn^{2+}$  at different initial concentrations as a function of contact time. It should be noted that the removal ratio of  $Mn^{2+}$  is increased with contact time and finally attained equilibrium under different initial concentrations (10 and 50 mg/L) at room temperature.

It can be observed from the figure that increasing the initial  $Mn^{2+}$  concentration will decrease the removal ratio of  $Mn^{2+}$ . These happen due to saturation of the adsorbate into the adsorbent and less of binding sites. At lower concentration (10 mg/L)  $Mn^{2+}$  molecules were adsorbed on the outer surface, but further increases in initial  $Mn^{2+}$  concentration (50 mg/L) led to fast saturation of adsorbent and thus most of the  $Mn^{2+}$  adsorption took place slowly inside the pores. From the results, the minimum and maximum time was determined (0.5 and 6 h).

### 3.3. Effect of pH at fixed contact time and adsorbent weight

The influence of pH on the adsorption of  $Mn^{2+}$  was investigated at different pH values ranging from 2.0 to 8.0 (Fig. 3). As the pH increased (from 2 to 5), the overall surface charge of adsorbent became negative and removal ratio of  $Mn^{2+}$  increased. As can be seen from the figure, the removal of metal ions from aqueous solution was strongly affected by medium pH. It can be noted that at low initial pH, the removal of  $Mn^{2+}$  is low. This happened due to the competition between the  $H_3O^+$  ion and  $Mn^{2+}$  ion to fill the surface of the adsorbent. For pH more than 5.0 the metal cations begin to precipitate (decreases with acidity increasing metal cations precipitated (reaction 2)). This reduces the concentration of  $Mn^{2+}$  in the solution and thus decreases the removal ratio of adsorbent.



### 3.4. Statistical analysis

A theoretical model was introduced for prediction and investigation of factor importance in determining of the removal ratio of  $Mn^{2+}$ . For this order, SPSS software (v. 19) in backward mode was employed and its obtained ANOVA table was investigated after development multi-

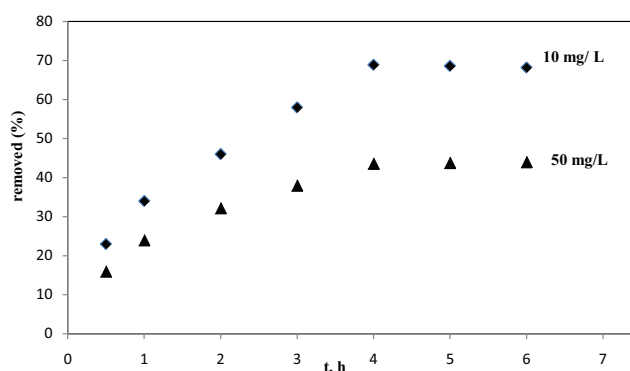


Fig. 2. Effect of contact time and initial concentration on the removal ratio of  $Mn^{2+}$  ions at room temperature (adsorbent weight = 4 g).

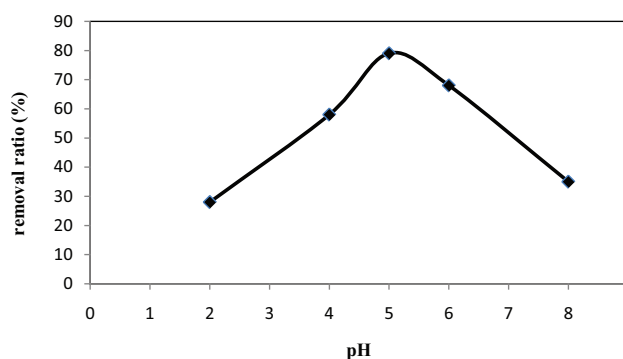


Fig. 3. Effect of pH on the removal ratio of  $Mn^{2+}$  ions at room temperature (adsorbent weight = 4 g, initial concentration = 10 mg/L,  $t = 4$  h).

ple linear regression (MLR) models [17]. Factors that were studied are: contact time, concentration of  $Mn^{2+}$ , adsorbent weight and pH of solution. According to the results of the batch experiments, minimum and maximum for each factor were determined. The average for each factor in theory calculated. These values (minimum, average and maximum) were shown with codes -1 0 1 (Box-Behnken Design). Then, using Box-Behnken statistical design, 27 experiments were designed. After conducting experiments designed and determine the removal ratio of  $Mn^{2+}$ , optimal parameters were calculated by SPSS software: concentration of  $Mn^{2+}$ : 10 mg/L, adsorbent weight: 2.5 g, time: 210 min, pH: 5.

For evaluation and selection of best model, R-value, standard error (SE) and F-value were compared between all of obtained MLR model. Finally, the model with greater R, fewer SE and greater F was selected (the fifth model). These parameters were reported in the Table 1.

For reviewing the importance of factors, the mean effect value as Beta-value was investigated. Beta-value of factors and characteristics of best model was shown in Table 2.

According to Beta-value in Table 2, the importance order of factors is: pH, W, C and t, respectively. It should be noted that the magnitude of Beta-value denotes the magnitude importance of the factor and the sign of Beta-value shows

Table 1  
Model summary

| Model | R                  | R <sup>2</sup> | Adjusted R <sup>2</sup> | Std. error of the estimate |
|-------|--------------------|----------------|-------------------------|----------------------------|
| 1     | 0.990 <sup>a</sup> | 0.980          | 0.956                   | 5.23804                    |
| 2     | 0.990 <sup>b</sup> | 0.980          | 0.960                   | 5.03255                    |
| 3     | 0.990 <sup>c</sup> | 0.980          | 0.963                   | 4.85938                    |
| 4     | 0.989 <sup>d</sup> | 0.979          | 0.963                   | 4.82589                    |
| 5     | 0.989 <sup>e</sup> | 0.977          | 0.963                   | 4.81812                    |
| 6     | 0.988 <sup>f</sup> | 0.975          | 0.962                   | 4.88836                    |
| 7     | 0.986 <sup>g</sup> | 0.973          | 0.960                   | 4.99592                    |
| 8     | 0.985 <sup>h</sup> | 0.970          | 0.959                   | 5.10504                    |

Table 2  
Characteristics of best model

| Coefficients |                 | Unstandardized coefficients |            | Standardized coefficients |  | t       |
|--------------|-----------------|-----------------------------|------------|---------------------------|--|---------|
| Model        |                 | B                           | Std. error | Beta                      |  |         |
| 5            | (constant)      | 63.113                      | 2.073      |                           |  | 30.440  |
|              | C               | -7.992                      | 1.391      | -0.216                    |  | -5.746  |
|              | W               | 12.010                      | 1.391      | 0.325                     |  | 8.635   |
|              | pH              | 15.904                      | 1.391      | 0.430                     |  | 11.435  |
|              | t               | 6.149                       | 1.391      | 0.166                     |  | 0.421   |
|              | CW              | 3.280                       | 2.409      | 0.051                     |  | 1.362   |
|              | WpH             | 6.250                       | 2.409      | 0.098                     |  | 2.594   |
|              | pHt             | 3.387                       | 2.409      | 0.053                     |  | 1.406   |
|              | W <sup>2</sup>  | -2.908                      | 1.967      | -0.059                    |  | -1.478  |
|              | pH <sup>2</sup> | -38.184                     | 1.967      | -0.770                    |  | -19.412 |
|              | t <sup>2</sup>  | 2.408                       | 1.967      | 0.049                     |  | 1.224   |

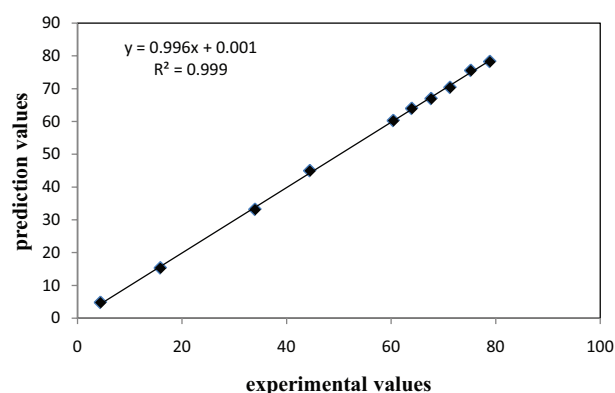
the direction of dependency of factor with target parameter (% Mn<sup>2+</sup>). A model which demonstrates the relationship between Mn<sup>2+</sup> removal ratio and independent variables is given in Eq. (3). The model is proposed based on the regression coefficients in Table 2.

$$\eta \% = 63.113 (\pm 2.073) - 7.992 (\pm 1.391)C + 12.010 (\pm 1.391)W + 15.904 (\pm 1.391)pH + 6.149 (\pm 1.391)t + 3.280 (\pm 2.409)CW + 6.250 (\pm 2.409)WpH + 3.387 (\pm 2.409)pHt - 2.908 (\pm 1.967)W^2 - 38.184 (\pm 1.967)pH^2 + 2.408 (\pm 1.967)t^2 \quad (3)$$

Also, the obtained results from this study show the good adaptation between experimental and prediction values of removal ratio of % Mn<sup>2+</sup>. Fig. 1 represents predicted vs. experimental values of removal ratio of Mn<sup>2+</sup>.

### 3.5. Adsorption isotherms of Mn<sup>2+</sup>

Several equilibrium adsorption isotherm models are available. Three isotherm models, Langmuir (1918), Freundlich, and Temkin (1940), employed to explore the adsorp-

Fig. 4. Plot of prediction of removal ratio of % Mn<sup>2+</sup> vs. experimental value of it.

tion mechanism. The adsorption isotherms were studied by varying the concentration of Mn<sup>2+</sup> solutions ranging from 10 to 50 mg/L with optimal amount of parameters (adsorbent weight: 2.5 g, time: 210 min, pH: 5).

### 3.6. Langmuir isotherm model

Langmuir equation is a semi-empirical isotherm derived from a proposed kinetic mechanism. It is based on four assumptions:

1. The surface of the adsorbent is uniform, that is, all the adsorption sites are equivalent.
2. Adsorbed molecules do not interact.
3. All adsorption occurs through the same mechanism.
4. At the maximum adsorption, only a monolayer is formed: molecules of adsorbate do not deposit on other, already adsorbed, molecules of adsorbate, only on the free surface of the adsorbent.

The linear equation of Langmuir isotherm model is expressed as follows:

$$\frac{C_e}{q_e} = \frac{C_e}{q_m} + \frac{1}{K_L q_m} \quad (4)$$

where  $q_m$  is the monolayer adsorption capacity of biosorbent (mg/g) and  $K_L$  is the Langmuir biosorption constant related to the energy of adsorption (L/mg). The values  $q_m$  and  $K_L$  were obtained from linear regression and presented in Table 3.

### 3.7. Freundlich isotherm model

Freundlich studied the sorption of a material onto animal charcoal. This fairly satisfactory empirical isotherm can be used for non ideal and multi-layer adsorption and is expressed by following equation:

$$\log q_e = \log K_F + \frac{1}{n} \log C_e \quad (5)$$

where  $K_F$  is the Freundlich constant related to the adsorption capacity ((mg/g)(l/mg)<sup>1/n</sup>), and  $n$  is the Freundlich

Table 3  
Langmuir, Freundlich, and Temkin constants

|                                       | Langmuir   |
|---------------------------------------|------------|
| $q_m$ (mg/g)                          | 1.92       |
| $K_L$ (L/mg)                          | 0.078      |
| $R_L^2$                               | 0.9647     |
|                                       | Freundlich |
| $n_F$                                 | 1.6455     |
| $K_F$ ((mg/g)·(L/mg) <sup>1/n</sup> ) | 0.195      |
| $R_F^2$                               | 0.999      |
|                                       | Temkin     |
| $B_T$                                 | 0.3938     |
| $K_T$ (L/mg)                          | 1.14       |
| $R_T^2$                               | 0.9574     |

exponent related to the intensity of adsorption or surface heterogeneity. Heterogeneity becomes more prevalent as  $1/n$  gets closer to zero. The values of  $K_F$  and  $1/n$  can be calculated from the plot of  $\ln q_e$  versus  $\ln C_e$  respectively.

### 3.8. Temkin isotherm model

The interaction of different adsorbates on the adsorbent was not considered in the Langmuir and Freundlich isotherms. Temkin and Pyzhev (1940) considered the effect of the adsorbate interaction on adsorption and proposed the model known as the Temkin isotherm, which can be expressed as,

$$q_e = B_T \ln K_T + B_T \ln C_e$$

$$B_T = \frac{RT}{b} \quad (6)$$

where  $K_T$  (L/mg) is Temkin isotherm energy constant and  $B_T$  is Temkin isotherm constant related to heat of sorption,  $R$  is the gas constant and  $T$  is the temperature. A plot of  $q_e$  versus  $\ln C_e$  is presented in Fig. 5.

These results indicate that Freundlich isotherm model still fits the data better.

### 3.9. Adsorption kinetics

Adsorption is a physicochemical process that involves the mass transfer of a solute (adsorbate) from the fluid phase to the adsorbent surface. A study of kinetics of adsorption is desirable as it provides information about the mechanism of adsorption, which is important for efficiency of the process. The applicability of the pseudo-first-order and pseudo-second-order model was tested for the adsorption of  $Mn^{2+}$  onto OFS. The best-fit model was selected based on the linear regression correlation coefficient,  $R^2$ , values.

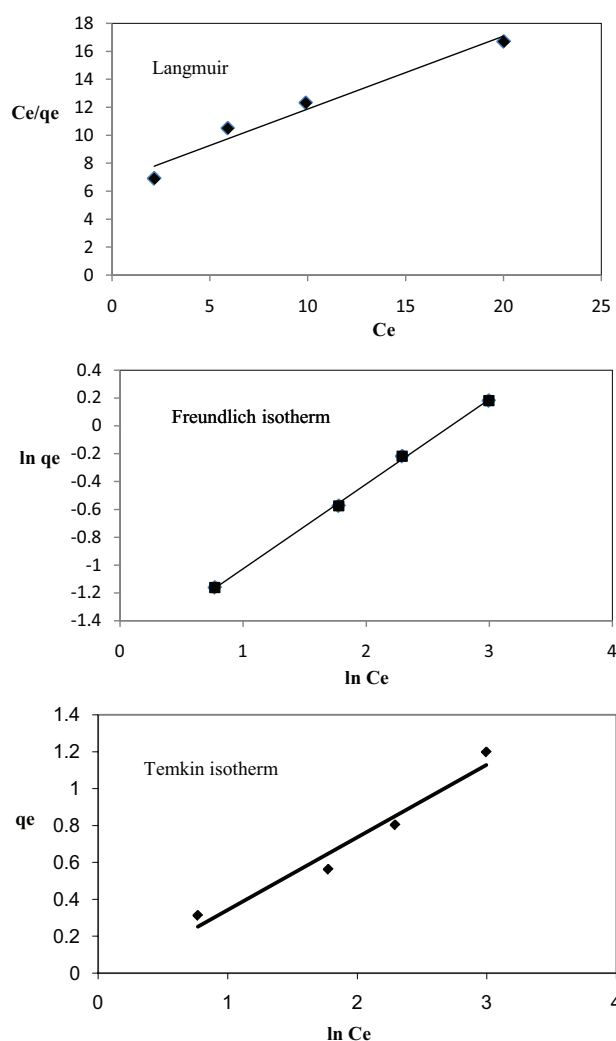


Fig. 5. Different isotherm plots for the adsorption of  $Mn^{2+}$ .

### 3.10. The first-order kinetic model

The Lagergren rate equation is one of the most widely used adsorption rate equations for the adsorption of solute from a liquid solution. The pseudo-first-order kinetic model of Lagergren may be represented by Lagergren:

$$\frac{dq_t}{dt} = k_1(q_e - q_t) \quad (7)$$

Integrating this equation for the boundary conditions  $t = 0$  to  $t = t$  and  $q = 0$  to  $q = q_t$ , gives:

$$\ln(q_e - q_t) = \ln q_e - k_1 t \quad (8)$$

where  $q_t$  is the amount of  $Mn^{2+}$  adsorbed (mg/g) at time  $t$  (min) and  $k_1$  is the rate constant of pseudo-first-order adsorption (1/min). The validity of the model can be checked by linearized plot of  $\ln(q_e - q_t)$  versus  $t$ . The rate constant of pseudo-first-order adsorption is determined from the slope of the plot (Fig. 6 and Table 4).

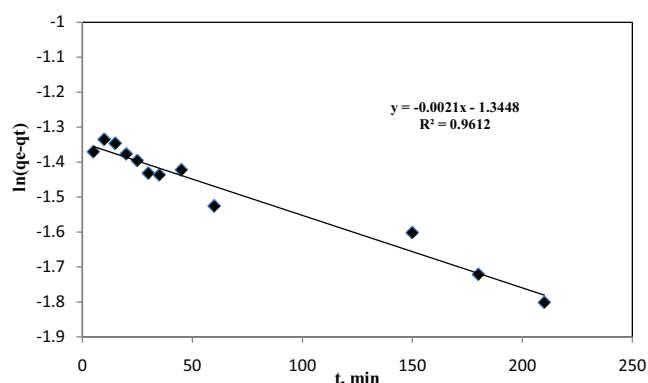


Fig. 6. Pseudo-first-order kinetic model.

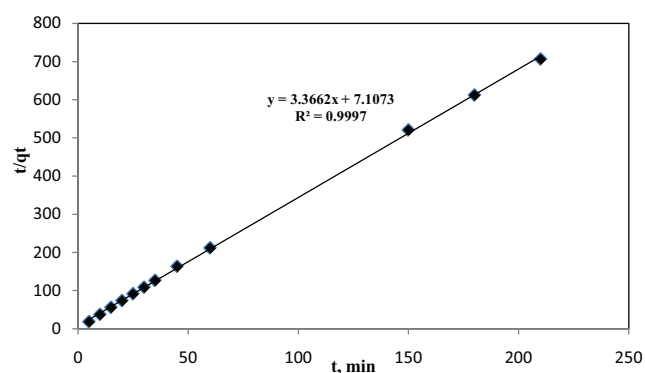


Fig. 7. Pseudo-second-order kinetic model.

Table 4  
Kinetic parameters

| Kinetic models           | Parameters                       |        |
|--------------------------|----------------------------------|--------|
| Pseudo-first-order       | $q_{e,cal}$ (mg/g)               | 0.26   |
|                          | $k_1$ (l/min)                    | 0.0021 |
|                          | $R^2$                            | 0.9612 |
| Pseudo-second-order      | $q_{e,cal}$ (mg/g)               | 0.297  |
|                          | $k_2$ (l/min)                    | 0.039  |
|                          | $R^2$                            | 0.9997 |
| Intra-particle-diffusion | $K_d$ (mg/g·min <sup>1/2</sup> ) | 0.0025 |
|                          | $R^2$                            | 0.9785 |
|                          | $q_{e,cal}$ (mg/g)               | 0.2598 |

### 3.11. The pseudo-second-order kinetic model

The pseudo-second-order kinetic model is expressed as follows:

$$\frac{dq_t}{dt} = k_2 (q_e - q_t)^2 \quad (9)$$

Rearranging the variables in Eq. (9) gives

$$\frac{dq_t}{(q_e - q_t)^2} = k_2 dt \quad (10)$$

Taking into account, the boundary conditions  $t = 0$  to  $t = t$  and  $q = 0$  to  $q = q_t$ , the integrated linear form of Eq. (10) can be rearranged to obtain Eq. (11):

$$t / q_t = 1 / k_2 q_e^2 + t / q_e \quad (11)$$

where the equilibrium adsorption capacity ( $q_e$ ), and the second order constant  $k_2$  (g/mg·min) can be determined experimentally from the slope and intercept of plot  $t/q_t$  vs.  $t$  [18] (Fig. 7 and Table 4).

The linear plot of  $t/q_t$  versus  $t$  show good agreement between experimental ( $q_{e,exp} = 0.31$  mg/g) and calculated ( $q_{e,cal}$ ) values (Table 4). At an initial  $Mn^{2+}$  concentration of 10 mg/L, the correlation coefficient for the second-order kinetics model ( $R^2$ ) is higher than 0.999. These results confirm

that the adsorption data were well represented by the pseudo-second-order kinetic model.

### 3.12. Adsorption mechanism

The predication of the rate-limiting step is an important factor to be considered in sorption process. For solid-liquid sorption, the process was usually characterized by either external mass transfer (boundary layer diffusion) or intra-particle diffusion or both.

### 3.13. Intraparticle diffusion

The adsorbate species are most probably transported from the bulk of the solution into the solid phase through an intraparticle diffusion process, which is often the rate limiting step in many adsorption processes. The possibility of intraparticle diffusion was explored by using the intraparticle diffusion model. An empirically found functional relationship, common to the adsorption processes defines that the uptake varies almost proportionally with  $t_{1/2}$ , the Weber-Morris plot, rather than with the contact time  $t$ :

$$q_t = k_d \sqrt{t} \quad (12)$$

where  $k_d$  is intraparticle diffusion rate constant (mg/g·min<sup>1/2</sup>). If the straight line passes through the origin, then intraparticle diffusion is the rate controlling step [19]. Otherwise, the intraparticle diffusion is not the only rate-limiting step, suggesting that the process is controlled by more than one mechanism limiting the rate of sorption. The intraparticle diffusion plot is given in Fig. 8. In the present study, it is showed that the adsorption process was linear over the whole time and the line has nonzero intercept. This revealed that the coexistence of boundary layer diffusion and intraparticle diffusion during the adsorption process [20–22].

A comparison of the removal ratio of  $Mn^{2+}$  ions onto different adsorbents is given in Table 5. As seen, the removal ratio of  $Mn^{2+}$  ions higher than that of reported adsorbents [9,12,14,16]. This may be attributed to effect of surface area, morphology, surface structure and functional groups. However, higher adsorption capacities of  $Mn^{2+}$

have been reported by other researchers [11,13,15]. Nonetheless, this comparison is not precise, since the experimental conditions are different. This result reveals that the Iranian oak-fruit shell is effective adsorbent for  $Mn^{2+}$  ions from wastewater due to its low cost and friendly environmental adsorbent.

### 3.14. FT-IR Spectroscopy

The FT-IR technique was an important tool to identify some important functional groups, which are capable of adsorbing pollutant ions [23]. The FT-IR spectra before and after sorption of  $Mn^{2+}$  is shown in Fig. 9. The spectra of adsorbent was measured within the range of 400–4000  $cm^{-1}$  wave number. The adsorption bands at 3388  $cm^{-1}$  and 2913 are assigned to O–H bonds (stretch) and C–H bonds (stretch), respectively [22,24]. The peak is wide because the polarity of hydroxyl groups is strong (2500–3500  $cm^{-1}$ ).

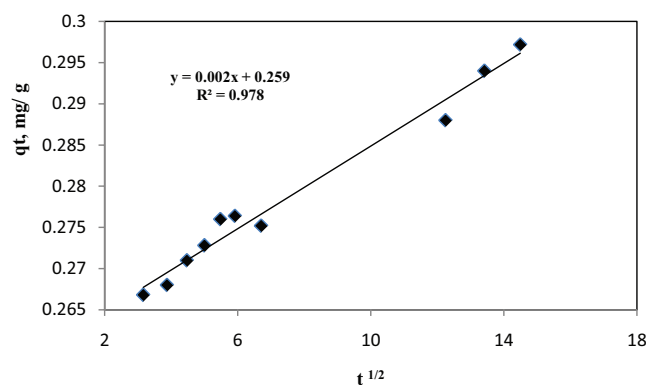


Fig. 8. Intraparticle diffusion plot.

Peaks observed at 1712 and 1596  $cm^{-1}$  are due to C=O stretching vibrations and carboxylate bands. In addition the bands of 1422 and 1485  $cm^{-1}$  confirm the presence of C=C of aromatic rings. Several bands ranging from 1010–1345  $cm^{-1}$  refer to C–O bonding. The peak at 568  $cm^{-1}$  represents O–C–O scissoring. The adsorption peak intensity and vibrational frequency change in the functional groups on spectrum of the adsorbent before adsorption comparing with after adsorption indicating that  $Mn^{2+}$  was adsorbed on functional group of the adsorbent.

### 3.15. Scanning electron microscope (SEM)

In order to elucidate the particle properties (e.g., surface morphology and particle size) of the oak-fruit shell, the particle texture was observed by the scanning electron microscope (Fig. 10). Prior to the observation, the surface

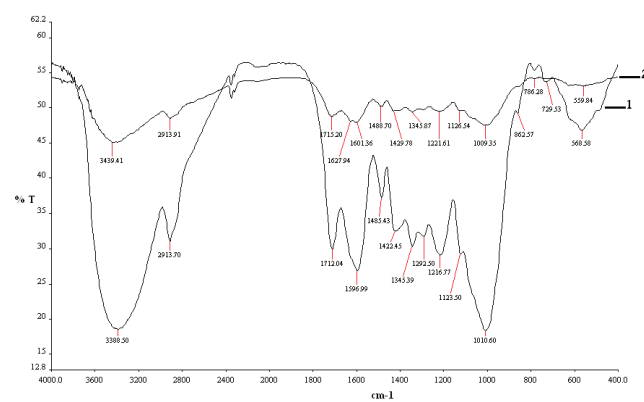


Fig. 9. FT-IR spectrum of OFS before (1) and after (2)  $Mn^{2+}$  adsorption.

Table 5  
The removal ratio of  $Mn^{2+}$  by different type of adsorbents

| Adsorbent                                   | Operating conditions   | The removal ratio | Reference  |
|---|--|-------------------|------------|
| Iranian oak-fruit shell (OFS)               | T = 20°C, W = 2.5 g, C = 10 mg/L, t = 210 min, pH = 5                                  | $\eta = 73.59\%$  | This study |
| Sargassum biomass                           | T = 23 °C, W = 3 g/L, C = 10 mg/L, t = 3 h, pH = 6, agitation rate = 150 rpm           | $\eta = 55.1\%$   | [9]        |
| Polyvinyl alcohol/chitosan (PVA/CS)         | T = 30°C, W = 0.8 g/100 mL, C = 20 mg/L, t = 120 min, pH = 6, agitation rate = 200 rpm | $\eta = 83.5\%$   | [11]       |
| Co/Mo layered double hydroxide (Co/Mo-LDH)  | T = 298 K, W = 0.2 g/1.0 L, C = 145 mg/L, t = 60 min, pH = 5                           | $\eta = 28\%$     | [12]       |
| Activated carbon from coconut shells (ACCS) | T = 298 K, W = 0.03 g/100 mL, C = 20 mg/L, t = 60 min, pH = 5.8                        | $\eta = 85\%$     | [13]       |
| Aerobic activated sludge                    | T = 20°C, W = 0.2 g/10 mL, C = 50 mg/L, t = 6 h, pH = 5, agitation rate = 150 rpm/min  | $\eta = 45\%$     | [14]       |
| Aerobic activated sludge                    | T = 20°C, W = 0.2 g/100 mL, C = 50 mg/L, t = 6 h, pH = 5, agitation rate = 150 rpm/min | $\eta = 40\%$     | [14]       |
| Enhanced empty fruit bunch (EFB)            | T = 26°C, W = 5 g/100 mL, C = 2.14 mg/L, t = 60 min, pH = 8.56                         | $\eta = 93.6\%$   | [15]       |
| White rice husk ash                         | T = 298 K, W = 1.5 g/L, C = 10 mg/L, t = 120 min, pH = 7                               | $\eta = 25\%$     | [16]       |



Fig. 10. SEM of OFS.

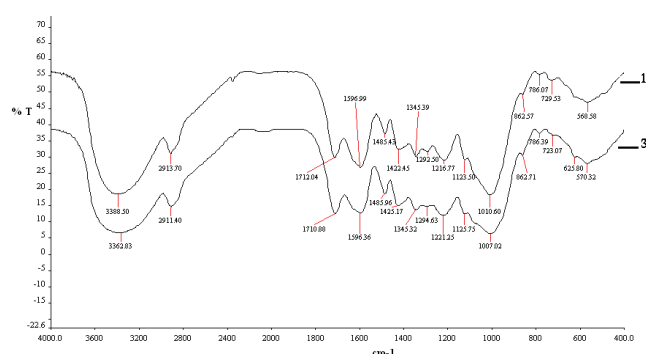


Fig. 11. FT-IR spectrum of OFS(1) and OFS regenerated (3).

of the sample was coated with a thin, electric conductive gold film. The SEM image revealed the nature of the surface of this biosorbent as a multilayer porous surface with irregular laminated structure, which may be beneficial to metal ions diffusion and adsorption. As can be seen from the figure, generally, the particles are spherical in different sizes.

### 3.16. The regeneration studies

Regeneration of adsorbent is important aspect to minimize the waste and reuse of the adsorbent. Reuse of adsorbent for adsorption of  $Mn^{2+}$  in optimal conditions demonstrated that adsorbent can be used for adsorption and removal ratio of  $Mn^{2+}$  was reduced to 63%. The results reveal that OFS can be potentially reused for further adsorption process. Fig. 11, FT-IR spectrum of the OFS and OFS recycled has been compared. Fig. 11 suggests that FT-IR spectrums are compatible with each other.

## 4. Conclusion

The Iranian oak-fruit shell employed in the adsorption process is efficient in removing  $Mn^{2+}$  from aqueous solutions. The removal ratio of  $Mn^{2+}$  from aqueous solutions was found to increase with an increase in pH, time and

adsorbent weight. On the contrary, with rising of initial  $Mn^{2+}$  concentration, the removal ratio decreased. Adsorption equilibrium was better described by the Freundlich isotherm model than the Langmuir and Temkin models. The SPSS analysis results showed that the importance order of factors is: pH of solution, adsorbent weight, initial  $Mn^{2+}$  concentration and time respectively. Also, the obtained results from this study show the good adaptation between experimental and prediction values of removal ratio of  $Mn^{2+}$ . Pseudo-second-order kinetic model agrees very well with the experimental data. The desorption and regeneration studies have proven that adsorbent can be potentially reused for further adsorption process.

## Acknowledgments

The authors thank the Golestan University for providing financial support of the work described in this paper.

## References

- [1] N. Gupta, Equilibrium and kinetics studies of Chromium (VI) ions adsorption on to carrot residue from aqueous solutions, *Asian J. Biochem. Pharm. Res.*, 2 (2012) 229–240.
- [2] F. Fu, Q. Wang, Remove of heavy metal ions from waste waters: a review, *J. Environ. Manage.*, 92 (2011) 407–418.
- [3] A. Ahmadi, Sh. Heidarzadeh, A.R. Mokhtari, E. Darezereshki, H. Asadi Harouni, Optimization of heavy metal removal from aqueous solutions by maghemite ( $\gamma\text{-Fe}_2\text{O}_3$ ) nanoparticles using response surface methodology, *J. Geochem. Explor.*, 147 (2014) 151–158.
- [4] N.N. Nassar, Rapid removal and recovery of Pb (II) from wastewater by magnetic Nano adsorbents, *J. Hazard. Mater.*, 184 (2010) 538–546.
- [5] Z.A. Al Othman, M.A. Habila, R. Ali, A.A. Ghafar, M.S. El-din Hassouna, Valorization of two waste streams into activated carbon and studying its adsorption kinetics, equilibrium isotherms and thermodynamics for methylene blue removal, *Arab. J. Chem.*, 7 (2014) 1148–1158.
- [6] Z.A. Al Othman, M.A. Habila, A. Hashem, Removal of zinc (II) from aqueous solutions using modified agricultural wastes: kinetics and equilibrium studies, *Arab. J. Geosci.*, 6 (2013) 4245–4255.
- [7] Z.A. Al Othman, A. Hashem, M.A. Habila, Kinetics, equilibrium and Thermodynamics studies of Cadmium (II) adsorption by modified agricultural wastes, *Molecules*, 16 (2011) 10443–10456.
- [8] V.B.H. Dang, H.D. Dogan, T. Dang-Vu, A. Lohi, Equilibrium and kinetics of biosorption of cadmium (II) and copper (II) ions by Wheat Straw, *Biores. Technol.*, 100 (2009) 211–219.
- [9] K. Vijayaraghavan, T.T. Teo, R. Balasubramanian, U.M. Joshi, Application of sargassum biomass to remove heavy metal ions from synthetic multi-metal solutions and urban storm water runoff, *J. Hazard. Mater.*, 164 (2009) 1019–1023.
- [10] A.I. Adeogun, A.E. Ofudje, M.A. Idowu, S.O. Kareem, Equilibrium, kinetics and thermodynamics studies of the biosorption of Mn (II) ions from aqueous solution by raw and acid-treated corncob biomass, *BioResources*, 6 (2011) 4117–4134.
- [11] Z. Abdeen, S.G. Mohammad, M.S. Mahmoud, Adsorption of Mn (II) ion on Polyvinyl alcohol/chitosan dry blending from aqueous solution, *Environ. Natotech. Monit. Manage.*, 3 (2015) 1–9.
- [12] A.A. Bakr, M.S. Mostafa, E.A. Sultan, Mn (II) removal from aqueous solutions by Co/Mo layered double hydroxide: kinetics and thermodynamics, *Egypt. J. Petroleum*, 25 (2016) 171–181.

- [13] J.C. Moreno-Pirajan, V.S. Garcia-Cuello, L. Giraldo, The removal and kinetic study of Mn, Fe, Ni and Cu ions from wastewater onto activated carbon from coconut shells, *Adsorption*, 17 (2011) 505–514.
- [14] Y. Wu, J. Zhou, Y. Wen, L. Jiang, Y. Wu, Biosorption of heavy metal ions ( $\text{Cu}^{2+}$ ,  $\text{Mn}^{2+}$ ,  $\text{Zn}^{2+}$ , and  $\text{Fe}^{3+}$ ) from aqueous solutions using activated sludge: Comparison of aerobic activated sludge with anaerobic activated sludge, *Appl Biotechnol.*, 168 (2012) 2079–2093.
- [15] M.K. Aмоса, Process optimization of Mn and  $\text{H}_2\text{S}$  removals from POME using an enhanced empty fruit bunch (EFB)-based adsorbent produced by pyrolysis, *Environ. Nanotech. Monit. Manage.*, 4 (2015) 93–105.
- [16] M.P. Tavlieva, S.D. Genieva, V.G. Georgieva, L.T. Vlaev, Thermodynamics and kinetics of the removal of manganese (II) ions from aqueous solutions by white rice husk ash, *J. Molecular. Liquids.*, 211 (2015) 938–947.
- [17] SPSS/PC, Statistical Package for IBMPC, Quiad software, Ontario(1986).
- [18] Y.S. Ho, G. McKay, The kinetics of sorption of basic dyes from aqueous solution by sphagnum moss peat, *Can. J. Chem. Eng.*, 76 (1998) 822–827.
- [19] Y.S. Ho, Removal of copper ions from aqueous solution by tree fern, *Water Res.*, 37 (2003) 2323–2330.
- [20] E. Rubin, P. Rodriguez, R. Herrero, M.E. Sastre de Vicente, Adsorption of methylene blue on chemically modified algal biomass: equilibrium, dynamic, and surface data, *J. Chem. Eng. Data.*, 55 (2010) 5707–5714.
- [21] K.V. Kumar, A. Kumaran, Removal of methylene blue mango seed kernel powder, *Biochem. Eng. J.*, 27 (2005) 83–93.
- [22] L. Ma, Y. Peng, B. Wu, D. Lei, H. Xu, Pleurotus *Ostreatus* nanoparticles as a new nano-biosorbent for removal of Mn (II) from aqueous solution, *Chem. Eng. J.*, 225 (2013) 59–67.
- [23] R.P. Han, L. Zhang, Ch. Song, M. Zhang, H. Zhu, L. Zhang, Characterization of modified wheat Straw, kinetic and equilibrium study about copper ion and methylene blue adsorption in batch mode, *Carbohydr. Polym.*, 79 (2011) 1140–1149.
- [24] D.L. Pavia, G.M. Lampman, G.S. Kriz, *Introduction to Spectroscopy*, 2nd ed, Saunders Golden Sunburst Series, New York(1996).